

Article

Synthesis, Characterization, and Activity of Hydroxymethylnitrofurazone Nanocrystals against *Trypanosoma cruzi* and *Leishmania* spp.

Cauê Benito Scarim ^{1,*}, Aline de Souza ², Débora Soares Souza Marins ², Elda Gonçalves dos Santos ³, Lívia de Figueiredo Diniz Castro ³, Ivo Santana Caldas ³, Patrícia Ferreira Espuri ³, Marcos José Marques ³, Elizabeth Igne Ferreira ², Nadia Araci Bou-Chacra ² and Chung Man Chin ^{1,4}

¹ Department of Drugs and Medicines, School of Pharmaceutical Sciences, São Paulo State University (UNESP), Araraquara 14800-903, SP, Brazil

² Department of Pharmacy, School of Pharmaceutical Sciences, São Paulo University (USP-SP), São Paulo 05508-000, SP, Brazil

³ Department of Pathology and Parasitology, Federal University of Alfenas (UNIFAL-MG), Alfenas 37130-000, MG, Brazil

⁴ Advanced Research Center in Medicine, School of Medicine, Union of the Colleges of the Great Lakes (UNILAGO), São José do Rio Preto 15030-070, SP, Brazil

* Correspondence: caue.scarim@unesp.br; Tel.: +55-(16)-3301-6971



Citation: Scarim, C.B.; de Souza, A.; Marins, D.S.S.; Santos, E.G.d.; de Figueiredo Diniz Castro, L.; Caldas, I.S.; Espuri, P.F.; Marques, M.J.; Ferreira, E.I.; Bou-Chacra, N.A.; et al. Synthesis, Characterization, and Activity of Hydroxymethylnitrofurazone Nanocrystals against *Trypanosoma cruzi* and *Leishmania* spp. *Drugs Drug Candidates* **2022**, *1*, 43–55. <https://doi.org/10.3390/ddc1010005>

Academic Editor: Jean Jacques Vanden Eynde

Received: 20 October 2022

Accepted: 1 December 2022

Published: 13 December 2022

Publisher's Note: MDPI stays neutral with regard to jurisdictional claims in published maps and institutional affiliations.



Copyright: © 2022 by the authors. Licensee MDPI, Basel, Switzerland. This article is an open access article distributed under the terms and conditions of the Creative Commons Attribution (CC BY) license (<https://creativecommons.org/licenses/by/4.0/>).

Abstract: Hydroxymethylnitrofurazone (NFOH) is a prodrug of nitrofurazone devoid of mutagenic toxicity, with in vitro and in vivo activity against *Trypanosoma cruzi* (*T. cruzi*) and in vitro activity against *Leishmania*. In this study, we aimed to increase the solubility of NFOH to improve its efficacy against *T. cruzi* (Chagas disease) and *Leishmania* species (Leishmaniasis) highly. Two formulations of NFOH nanocrystals (NFOH-F1 and NFOH-F2) were prepared and characterized by determining their particle sizes, size distribution, morphologies, crystal properties, and anti-trypanosomatid activities. Furthermore, cytotoxicity assays were performed. The results showed that the optimized particle size of 108.2 ± 0.8 nm (NFOH-F1) and 132.4 ± 2.3 nm (NFOH-F2) increased the saturation solubility and dissolution rate of the nanocrystals. These formulations exhibited moderate anti-*Leishmania* effects (*Leishmania amazonensis*) in vitro and potent in vitro activity against *T. cruzi* parasites (Y strain). Moreover, both formulations could reduce parasitemia (around 89–95% during the parasitemic peak) in a short animal model trial (Y strain from *T. cruzi*). These results suggested that the increased water solubility of the NFOH nanocrystals improved their activity against Chagas disease in both in vitro and in vivo assays.

Keywords: antikinoplastid; nanotechnology; drug discovery

1. Introduction

American trypanosomiasis (Chagas disease) and leishmaniasis are considered neglected tropical diseases (NTDs) and represent a severe global health problem. These two NTDs, caused by the protozoans *Trypanosoma cruzi* and *Leishmania* spp., respectively, affect approximately 10 million people worldwide and are responsible for more than 44,000 deaths per year [1,2]. Available treatments for these NTDs still rely on decades-old drugs. Most of these drugs are toxic, show decreasing efficacy, and exhibit several side effects. They also involve a complicated route of administration and require patient compliance [3–11]. Therefore, discovering and developing novel, effective, safe, and affordable anti-trypanosomatid agents are a high priority [12,13].

Hydroxymethylnitrofurazone (NFOH) is a nitrofurazone prodrug (Figure 1), which has been considered a crucial and promising anti-*T. cruzi* candidate in vitro [14,15]. Its activity was evaluated and confirmed in murine models with acute and chronic stages of Chagas disease [15–17]. Moreover, the Ames test confirmed the absence of mutagenic toxicity in

NFOH [14]. Furthermore, no hepatotoxicity was presented by NFOH when administered in Balb/c mice for a long period (60 days) in high concentrations (150 mg/kg) [17,18].

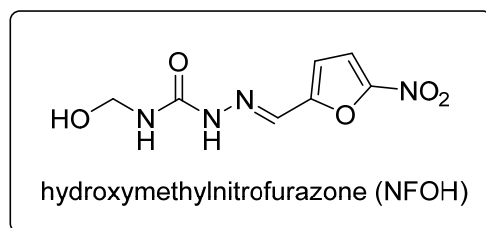


Figure 1. Chemical structure of hydroxymethylnitrofurazone (NFOH).

Developing nanocrystal-based pharmaceutical products has increased in the last few decades. The Food and Drug Administration received more than 80 submissions of nanocrystal-containing drugs by the year 2016 that could be administered by different routes and for several diseases [19]. Nanocrystals are carrier-free drug particles prepared in dispersion media using stabilizers (surfactants or polymers), resulting in a colloidal system [20]. The stabilization (steric, electrostatic, or electrosteric) can minimize the risk of nanoparticle agglomeration. These nanoparticles can improve the dissolution velocity and increase the saturation solubility of the drugs based on Noyes–Whitney equations [21]. Additionally, nanocrystals can increase the adhesiveness of the biological membranes and the surface of the gastrointestinal tract compared with micrometer particles [20].

The preparation and physicochemical characterization of the NFOH nanocrystals (NFOH-F1 and NFOH-F2) presented in this study were proposed as an approach to obtain active targeted drug delivery against *T. cruzi* (Y strain) and *Leishmania amazonensis* (*L. amazonensis*), improving their in vitro activity against these trypanosomatid parasites. Moreover, due to potential anti-*T. cruzi* effects, the Chagas-murine model was evaluated for five day-treatment.

2. Results and Discussion

2.1. Screening for the Preparation of NFOH Nanocrystals

Formulations were screened based on the presence of monomodal distribution and the presence of precipitates, as they indicate the physical stability of the nanosuspension. Formulations F1 (particle size = 108.2 ± 0.8 nm) and F2 (particle size = 132.4 ± 2.3 nm) showed a monomodal distribution. The polydispersity indices (PI) for F1 and F2 were 0.281 ± 0.015 and 0.270 ± 0.002 , respectively. Thus, the formulations F1 and F2 were accepted, and F3, F4, F5, and F6 were rejected. Poloxamer 188 (P188) and poloxamer 407 (P407) surfactants were used to prepare NFOH-F1 and NFOH-F2 nanocrystals, respectively.

2.2. Factorial Design

Eleven experiments were performed corresponding to a factorial design employing three two-level factors (2^3) to evaluate the effect of independent variables. Table 1 shows the mean particle size (MPS), PI, and zeta potential (ZP) results obtained for these 11 experiments using P407. MPS and PI ranged from 191.3 ± 2.1 to 326.8 ± 4.6 nm and 0.21 ± 0.01 to 0.50 ± 0.01 , respectively. ZP ranged from -23.9 ± 0.7 to -30.8 ± 2.2 mV.

Table 1. Matrix of the response surface test using poloxamer 407 as a surfactant for mean particle size, polydispersity index, and zeta potential of the hydroxymethylnitrofurazone nanocrystals.

Formula	Order	Central Point	Time (hours)	NFOH (%w/w)	P407 (%w/w)	MPS	PI	ZP
1	1	1	48	3.0	1.0	248.2 ± 1.2	0.39 ± 0.01	-26.2 ± 0.5
2	2	0	84	2.0	2.0	271.0 ± 1.8	0.28 ± 0.02	-27.4 ± 0.2
3	3	1	120	3.0	1.0	191.3 ± 2.1	0.32 ± 0.04	-28.1 ± 1.4
4	4	0	84	2.0	2.0	278.3 ± 2.4	0.24 ± 0.01	-32.1 ± 2.3

Table 1. Cont.

Formula	Order	Central Point	Time (hours)	NFOH (%w/w)	P407 (%w/w)	MPS	PI	ZP
5	5	1	48	3.0	3.0	254.1 ± 6.7	0.41 ± 0.06	−25.5 ± 1.5
6	6	1	120	1.0	1.0	197.2 ± 0.5	0.25 ± 0.01	−30.8 ± 2.2
7	7	1	120	1.0	3.0	214.4 ± 1.4	0.24 ± 0.02	−23.9 ± 0.7
8	8	0	84	2.0	2.0	264.0 ± 1.1	0.28 ± 0.01	−27.7 ± 0.2
9	9	1	120	3.0	3.0	284.6 ± 1.9	0.21 ± 0.01	−28.0 ± 1.2
10	10	1	48	1.0	1.0	326.8 ± 4.3	0.21 ± 0.01	−29.1 ± 0.9
11	11	1	48	1.0	3.0	258.6 ± 2.8	0.50 ± 0.01	−27.2 ± 0.8

Table 2 shows the analysis of variance (ANOVA) performed, and parameters with $p < 0.05$ ($\alpha = 0.05$) were considered significant. The linear model was significant ($p < 0.05$; $\alpha = 0.05$). Among the main factors, only the stirring time was significant ($p = 0.001$; $\alpha = 0.05$). The following interactions were significant: NFOH*P407, NFOH*Stirring time, and P407*Stirring time ($p < 0.05$, $\alpha = 0.05$). The coefficients revealed similar values: 99.36%, 97.86%, and 98.36%, respectively, for R-square (R^2), adjusted- R^2 [R^2 (adj)], and predicted R^2 [R^2 (pred)] of the adjusted model.

Table 2. Analysis of variance (ANOVA) for mean particle size using poloxamer 407 Abbreviations: DF = degree of freedom, SS = sequential sums of squares, MS = sequential mean squares, F-Value = value of the F distribution, and p -value = lack-of-fit adjustment.

	DF	SS (adj)	MS (adj)	F Value	p Value
Model	7	15,890.7	2270.10	66.27	0.003
Linear	3	5344.6	1781.53	52.01	0.004
NFOH %w/w	1	44.2	44.18	1.29	0.330
P407 %w/w	1	290.4	290.41	8.48	0.062
Stirring Time (h)	1	5010.0	5010.00	146.26	0.001
Interaction	3	92,268.3	3089.44	90.19	0.002
NFOH %w/w × P407 %w/w	1	2820.0	2820.00	82.33	0.003
NFOH %w/w × Stirring Time (h)	1	2715.8	2715.85	79.29	0.003
P407 %w/w × Stirring Time (h)	1	3732.5	3732.48	108.97	0.002
Curve	1	1277.8	1277.76	37.30	0.009
Error	3	102.8	4.25		
Lack of adjustment	1	0.5	0.50	0.01	0.930
Pure Error	2	102.3	51.13		
Total	10	15,993.4			

SD = 5.85263 $R^2 = 99.36\%$ R^2 (adj) = 97.86% R^2 (pred) = 98.36%

The assumption of normality was verified using the normal probability plot, residual versus adjustment graph, and histogram. The residual versus adjustment graph showed randomness in the distribution.

The model was described by Equation (1), which correlates the effect of each factor and their interactions with the MPS response. Two experiments were performed using different concentrations to verify the adequacy of the model equation (A) NFOH (2.5% m/m) and P407 (2.5% m/m) and (B) NFOH (1.5% m/m) and P407 (1.5% w/w), as shown on Table 3.

Equation (1).

$$\text{MPS} = 559.8 - 82.89 \text{ NFOH} - 81.93 \text{ P407} - 2.919 \text{ Agitation Time} + 18.78 \text{ NFOH} \times \text{P407} + 0.5118 \text{ NFOH} \times \text{Agitation Time} + 0.6 \text{ P407} \times \text{Agitation Time} \quad (1)$$

For P188, the same analyses were performed; however, the linear model did not adequately fit the data. Therefore, performing another statistical analysis to design an appropriate mathematical model for evaluating the experimental data was necessary in

which 6 axial points and 3 central points were added in the factorial design. Thus, the factors considered significant in the new analysis were NFOH concentration, stirring time, and P188 concentration.

Table 3. Observed and predicted mean particle size and polydispersity index results from the hydroxymethylnitrofurazone nanocrystals.

Formula	Predicted MPS (nm)	Observed MPS (nm)	PI
A	248.39	245.2 ± 1.4	0.29 ± 0.01
B	204.67	199.4 ± 2.3	0.26 ± 0.03
C	213.6 ± 2.0	215.46	0.34 ± 0.01
D	219.1 ± 2.3	222.33	0.28 ± 0.03

The results of the response surface study are shown in Table 4. The MPS ranged from 184.8 ± 0.5 to 325.9 ± 2.2 nm, PI from 0.21 ± 0.01 to 0.57 ± 0.01, and ZP ranged from −31.7 ± 1.1 to −40.3 ± 0.6 mV.

Table 4. Matrix of the response surface test using poloxamer 188 as a surfactant for mean particle size, polydispersity index, and zeta potential of the hydroxymethylnitrofurazone nanocrystals.

Formula	Order	Central	Time (hours)	NFOH (%w/w)	P188 (%w/w)	MPS (nm)	PI	PZ (mV)
1	1	1	48	3.0	1.0	285.9 ± 3.3	0.43 ± 0.02	−33.2 ± 0.5
2	2	0	84	2.0	2.0	304.0 ± 2.1	0.29 ± 0.03	−33.4 ± 0.7
3	3	1	120	3.0	1.0	184.8 ± 0.5	0.34 ± 0.04	−33.3 ± 1.1
4	4	0	84	2.0	2.0	298.3 ± 2.1	0.21 ± 0.01	−40.3 ± 0.6
5	5	1	48	3.0	3.0	274.8 ± 3.1	0.57 ± 0.01	−34.6 ± 1.1
6	6	1	120	1.0	1.0	193.5 ± 3.2	0.23 ± 0.01	−34.5 ± 1.1
7	7	1	120	1.0	3.0	203.0 ± 0.1	0.26 ± 0.01	−34.8 ± 1.5
8	8	0	84	2.0	2.0	310.1 ± 3.3	0.24 ± 0.02	−36.6 ± 0.7
9	9	1	120	3.0	3.0	194.3 ± 2.1	0.31 ± 0.03	−31.7 ± 1.1
10	10	1	48	1.0	1.0	296.5 ± 2.5	0.22 ± 0.01	−38.7 ± 0.6
11	11	1	48	1.0	3.0	311.8 ± 2.2	0.39 ± 0.02	−38.2 ± 1.2
12	12	−1	120	2.0	2.0	198.5 ± 1.4	0.24 ± 0.04	−34.5 ± 1.4
13	13	0	84	2.0	2.0	298.3 ± 2.1	0.37 ± 0.07	−34.5 ± 0.6
14	14	−1	120	2.0	1.0	171.0 ± 0.7	0.22 ± 0.01	−36.3 ± 0.7
15	15	−1	84	3.0	1.0	194.4 ± 1.6	0.25 ± 0.01	−36.1 ± 0.6
16	16	0	84	2.0	2.0	299.3 ± 1.9	0.28 ± 0.02	−39.2 ± 0.9
17	17	1	48	2.0	1.0	256.1 ± 1.4	0.22 ± 0.03	−32.5 ± 0.2
18	18	−1	84	3.0	2.0	261.9 ± 2.1	0.29 ± 0.01	−31.7 ± 1.3
19	19	0	84	2.0	2.0	301.2 ± 2.7	0.32 ± 0.01	−38.1 ± 1.2
20	20	−1	84	1.0	1.0	217.9 ± 3.3	0.21 ± 0.02	−31.5 ± 1.8

Table 5 shows the ANOVA results for the MPS response. The quadratic model presented $p < 0.05$ ($\alpha = 0.05$). The coefficients revealed similar values: 98.00%, 97.29%, and 95.30%, respectively, for R^2 , R^2 (adj), and R^2 (pred) of the adjusted model. Furthermore, the lack of adjustment was not significant (0.051; $\alpha = 0.05$); therefore, the obtained model was considered statistically significant. The normal probability plot for residuals was approximately linear, revealing a normally distributed behavior. No heteroscedasticity phenomenon was observed. The graph of the individual observations showed the random behavior of the residuals (data not shown).

The model was described by Equation (2), which correlated the effect of each factor and their interactions with the MPS response. The coefficient for the term agitation time (h) contributed more efficiently to MPS reduction compared with NFOH concentration (% w/w), which was proved by the interaction of two factors (P188 [% w/w]*P188 [% w/w]) with negative coefficients.

Table 5. Analysis of variance for mean particle size using poloxamer 188 Abbreviations: DF = degrees of freedom, SS = sequential sums of squares, MS = sequential mean squares, F-Value = value on the F distribution, and * *p*-value = lack-of-fit adjustment.

	DF	SS (adj)	MS (adj)	F-Value	<i>p</i> -Value
Model	5	48,894.5	9778.9	137.46	0.001
Blocks	1	4318.6	4318.6	60.70	0.001
Linear	3	26,702.8	8900.9	125.12	0.001
NFOH % <i>w/w</i>	1	746.1	746.1	10.49	0.006
P188 % <i>w/w</i>	1	19.1	19.1	0.27	0.612
Stirring time (h)	1	26,149.6	26,149.6	367.57	0.001
Quadratic	1	14,030.0	14,030.0	197.21	0.001
P188 % <i>w/w</i> *P188 %	1	14,030.0	14,030.0	197.21	0.001
Error	14	996.0	71.1		
Lack of adjustment	9	891.2	99.0	4.72	0.051
Pure Error	5	104.8	21.0	*	*
Total	19	49,890.5			
SD = 8.43456	R ² = 98.00%	R ² (adj) = 97.29%	R ² (pred) = 95.30%		

Two experiments were performed using the following different concentrations to verify the adequacy of Equation 2 of the model: NFOH (2.5% *w/w*) and P188 (2.5% *w/w*) for **C** and NFOH (1.5% *m/m*) and P188 (1.5% *m/m*) for **D**, both with 120 h of stirring. Under these conditions, the MPS values observed in Table 5 were within the predicted value range, calculated with $\alpha = 0.05$. Thus, the result corroborated the validity of the mathematical model for MPS. The formulas selected for continuing the study are described in Table 6. They were selected because of their stability, and the MPS was less than 200 nm. Equation (2).

$$\text{MPS} = 188.2 - 8.35 \text{ NFOH} + 224.6 \text{ P188} - 1.3728 \text{ Agitation Time} - 55.78 \text{ P188} \times \text{P188} \quad (2)$$

Table 6. Selected formulas for characterizing in vitro and in vivo studies.

Formula	NFOH (% <i>w/w</i>)	Poloxamer 188 (% <i>w/w</i>)	Poloxamer 407 (% <i>w/w</i>)	Stirring Time (h)
NFOH-1	2.0	1.0	-	120
NFOH-2	3.0	-	1.0	120

Comparison between nanoparticle tracking analysis (NTA) and photon correlation spectroscopy (PCS) for particle size determination of NFOH nanocrystals. NTA is a technique for the visualization and direct real-time analysis of nanoparticles in liquids. Table 7 and Figure 2 show the particle sizes of the nanocrystals of NFOH.

Table 7. Particle size evaluation of the hydroxymethylnitrofurazone nanocrystals Abbreviations: NTA = nanoparticle tracking analysis, PCS = photon correlation spectroscopy, and MPS = mean particle size.

	NTA	MPS (nm)	
		NFOH-F1	NFOH-F2
	d (0,1)	91.3 ± 3.9	89.2 ± 0.1
	d (0,5)	136.7 ± 2.7	132.6 ± 6.4
	d (0,9)	188.2 ± 6.5	188.7 ± 4.5
	Mean	141.9 ± 0.6	138.2 ± 1.7
PCS	MPS	193.5 ± 3.2	197.2 ± 0.5

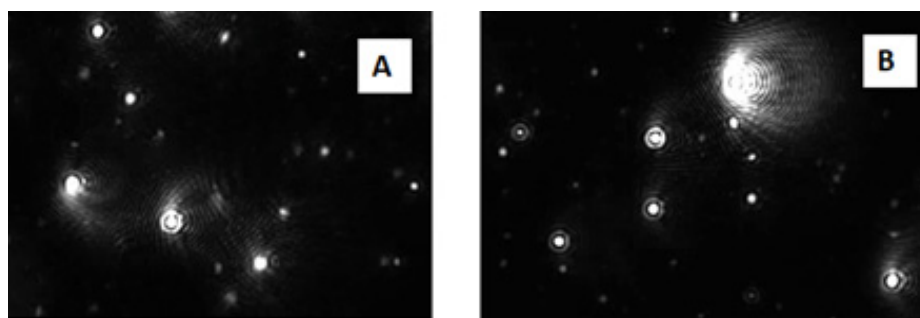


Figure 2. Hydroxymethylnitrofurazone (NFOH) nanocrystals by nanoparticle tracking analysis. (A): F-P188 (NFOH-F1); (B): F-P407 (NFOH-F2).

2.3. X-ray Diffraction (XRD)

NFOH crystallinity was previously determined by Doriguetto et al. (2005) [22]. XRD of NFOH and its nanosuspensions (Figure 3) showed characteristic peaks at 9.5° , 21.2° and 28.1° 2θ . Lyophilized NFOH nanocrystals characteristic peaks remained unchanged in the diffractograms with a decrease in peak height. The peak height is affected by crystal size and crystallinity [23]. These results showed that the adapted method of wet bead milling method was appropriated to prepare NFOH nanosuspensions.

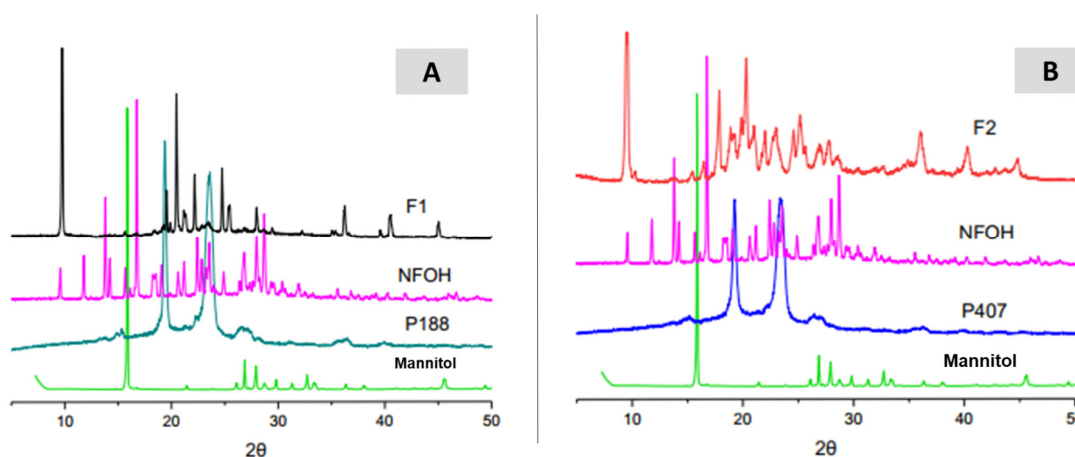


Figure 3. Diffractogram: (A) NFOH-1 (F1), NFOH, poloxamer 188 (P188), and mannitol; (B) NFOH-2 (F2), NFOH, poloxamer 407 (P407), and mannitol.

3. Biological Activity

3.1. Cytotoxicity on Macrophages (50.0% Cytotoxicity Concentrations [CC_{50}])

Both formulations presented low cytotoxicity to mouse peritoneal macrophage cells at tested concentrations (Tables 8 and 9). The CC_{50} values for peritoneal macrophage cells were 1194.7 and 885.5 μM for NFOH-F1 and NFOH-F2, respectively (Tables 8 and 9). The selectivity index analysis ($SI = CC_{50}/50.0\%$ inhibitory growth concentration [IC_{50}]) (Tables 8 and 9), which measured the selective toxicity extent of a compound to the parasites compared with a toxicity extent to the peritoneal macrophage cells of mice, showed that all evaluated compounds were more selective to the parasites than to the peritoneal macrophage cells.

Table 8. Anti-*Trypanosoma cruzi* activity (IC_{50} , μM) against epimastigote, trypomastigote, and amastigote forms (Y strain), cytotoxicity on peritoneal macrophage cells (CC_{50} , μM), and selectivity index ($[CC_{50}/IC_{50}]$) of hydroxymethylnitrofurazone (NFOH) formulations (NFOH-F1 and NFOH-F2) and benznidazole.

<i>T. cruzi</i> Y Strain	Cytotoxicity	Epimastigotes	Trypomastigotes	Amastigotes	
		SI		SI	SI
Compounds	CC50	IC50	IC50	IC50	
NFOH-F1	1194.7	11.02 +/- 2.4 108	8.9 +/- 0.3	134 2.29 +/- 0.95	521
NFOH-F2	885.5	18.83 +/- 4.06 47	10.5 +/- 0.56	84 4.85 +/- 3.91	182
Benznidazole	>300.0	8.01 +/- 1.31 >37	4.21 +/- 0.23	>71 4.8 +/- 1.7	>62

Table 9. Anti-leishmanial activity (IC_{50} , μM) against promastigote and amastigote forms (*Leishmania amazonensis*), cytotoxicity to peritoneal macrophage cells (CC_{50} , μM), and selectivity index (CC_{50}/IC_{50}) for hydroxymethylnitrofurazone formulations (NFOH-F1 and NFOH-F2) and amphotericin B.

<i>Leishmania</i> <i>amazonensis</i>	Cytotoxicity	Promastigotes	SI	Amastigotes	SI
	CC50				
Compounds					
NFOH-F1	1194.7	101.97 +/- 2.41	11.72	90.35 +/- 6.58	7.71
NFOH-F2	885.5	98.65 +/- 7.25	8.97	143.64 +/- 1.09	16.01
Amphotericin B	27.05	5.10 +/- 0.002	5.3	1.30 +/- 0.001	20.8

3.2. Anti-*T. cruzi* Activity (In Vitro)

The NFOH-F1 and NFOH-F2 formulations exhibited a high inhibition capacity, with IC_{50} values of 11.02 μM for NFOH-F1 (SI = 108) and 18.83 μM for NFOH-F2 (SI = 47) in *T. cruzi* epimastigote forms (Y strain, IC_{50} BZN = 8.01 μM) (Table 8). Moreover, NFOH-F1 and NFOH-F2 showed interesting values (IC_{50} = 8.9 and 10.5 μM ; SI = 134 and 84, respectively) against the blood trypomastigote forms of *T. cruzi* (Y strain) compared to frontline drug benznidazole (BZN) (IC_{50} BZN = 4.21 μM) (Table 8).

Both formulations (NFOH-F1 and NFOH-F2) presented potent values of IC_{50} (2.29 and 4.85 μM) and SI (521 and 182) against amastigote forms (Y strain), which showed promising results when compared with that of the standard drug BZN (IC_{50} = 4.8 μM) (Table 8). These are promising data considering the relevance of trypomastigote and amastigote human forms for treating Chagas disease.

3.3. Anti-Leishmanial Activity (In Vitro)

Both the formulations (NFOH-F1 and NFOH-F2) were evaluated against *Leishmania* ssp (Table 9). The tested formulations (NFOH-F1 and NFOH-F2) exhibited moderate activity against the promastigote (IC_{50} = 101.97 and 98.65 μM , SI = 11.72 and 8.97) and amastigote (IC_{50} = 90.35 and 143.64 μM , SI = 7.71 and 16.01) forms of *L. amazonensis* compared with amphotericin B (Table 9). Therefore, these formulations showed low cytotoxicity (1194.7 and 885.5 μM for NFOH-F1 and NFOH-F2, respectively) compared with amphotericin B (27.05 μM , Table 9). These data are important considering the relevance of current leishmania therapy.

3.4. Anti-*T. cruzi* Activity in Mice

Both formulations (NFOH-F1 and NFOH-F2) were administered to mice orally by gavage in a 5% Cremophor (Sigma) vehicle. Parasitemia was reduced in 100% of the animals treated with NFOH-F1 and NFOH-F2 or BZN. The area under the curve and

parasitemia peak were decrease in the group treated with NFOH-F1, and NFOH-F2 could be clearly observed during treatment (Figure 4). Mice receiving NFOH-F1 and NFOH-F2 showed a parasitemia peak with an order less than that of BZN (Figure 4). The animals showed normal habits, and no death was observed during the protocol.

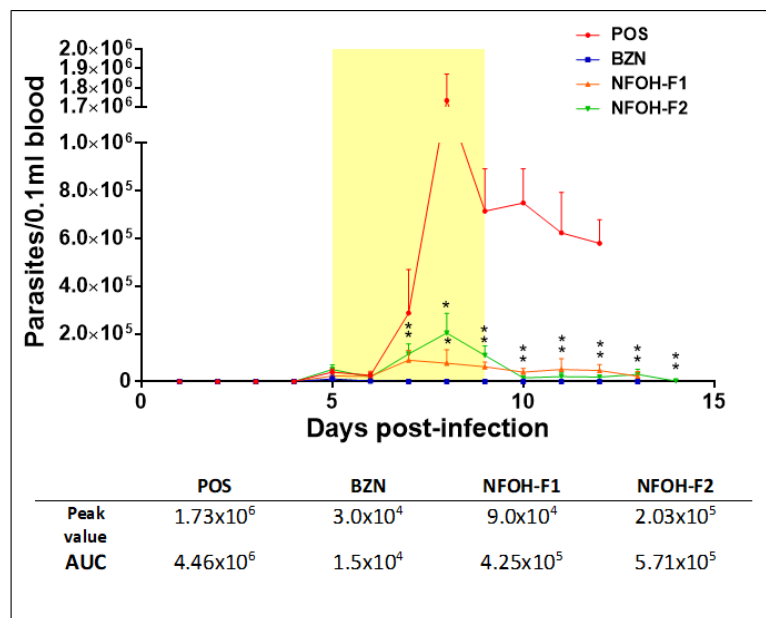


Figure 4. Effect on parasitemia of treatment with hydroxymethylnitrofurazone (NFOH)-F1, NFOH-F2, and BZN. The means of parasitemia values are represented by the lines. Yellow area: treatment period (5 days). POS: mice infected by *T. cruzi* and untreated; BZN: mice infected by *T. cruzi* and treated by BZN; NFOH-F1: mice infected by *T. cruzi* and treated by NFOH-F1; NFOH-F2: mice infected by *T. cruzi* and treated by NFOH-F2; Peak value: parasitemic peak (parasites); AUC: area under the curve; ** significant difference ($p < 0.05$).

We observed the improved anti-trypanosomatid activity after NFOH nanocrystal administration. Extensive studies have shown that nanosystems have the potential to be used for treating leishmaniasis [24] and Chagas disease [25]. The solubility and permeation of NFOH-F1 and NFOH-F2 were improved because of the increased superficial area, leading to increase bioavailability. A recent study using NFOH in another nanostructured polymeric system showed that it was 95-fold more active and exhibited SI values of about 50-fold compared with free NFOH when assayed against *L. amazonensis* amastigotes [26].

Both nanocrystal formulations (NFOH-F1 and NFOH-F2) exhibited anti-*T. cruzi* and anti-*L. amazonensis* activities in vitro. The effect against *T. cruzi* was potent and had similar IC_{50} values on all forms of the parasite, especially the amastigote forms. For these latter, the IC_{50} values were promising for NFOH-F1 and NFOH-F2 compared to BZN (Table 8), which were consequently tested in murine models. The in vivo results showed the ability of the nanocrystal formulations to eliminate blood parasitemia completely in the infected mice (Y strains-*T. cruzi*) (Figure 4). Thus, future studies should emphasize evaluating the capacity of these formulations to act on both stages of Chagas disease with low toxicity to consider NFOH as a safe drug.

4. Material and Methods

4.1. Chemistry

4.1.1. Preliminary Assay for Preparation of NFOH Nanocrystals

The nanocrystals of NFOH were prepared by the wet bead milling method adapted by Romero et al. (2016) [27]. The formulas were prepared using a small-scale system consisting of a glass grinding vessel (10 mL capacity), 0.1 mm (7.5 g) zirconium oxide

beads, and three cross bars. Different steric stabilizers were tested for preselecting those that allowed obtaining a preparation with MPS < 300 nm, PI < 0.3, and monomodal distribution immediately after preparation. Six formulas were prepared with 3.0% (*w/w*) of NFOH and 1.0% (*w/w*) of different surfactants (Polysorbate[®] 80 [Sigma-aldrich, San Luis, Missouri–EUA], Polysorbate[®] 20 [Sigma-aldrich, San Luis, Missouri–EUA], P188, P407, Kolliphor[®] HS 15 [BASF, Ludwigshafen–Germany], and Povacoat[®] [Daido Chemical Corporation, Osaka–Japan]) for 120 h at 800 rpm. The pH values of all formulas were adjusted to 7.5 using NaOH 0.1 M solution.

4.1.2. Factorial Design

After the preliminary tests, a factorial design was used to determine the important variables of the wet bead milling method and to obtain an appropriate mathematical model to describe the phenomenon. Two stabilizers, P188 and P407, were selected in the pre-selection stage. The independent variables selected were agitation time (h), NFOH concentration (% *w/w*), and surfactant concentration (% *w/w*). The responses or dependent variables were MPS, PI, and ZP. The amount of zirconium oxide beads (7.5 g) and the stirring speed (800 rpm) were constant for all formulations. The statistical analysis of the results obtained in the factorial design was performed using Minitab[®] 17.

4.1.3. MPS and PI Analysis

MPS and IP were determined using Zetasizer ZS90 (Malvern Instruments, Malvern, UK) by PCS at 25 °C and 90 °C. The samples were diluted in water to a suitable concentration. The particle size was determined by NTA. The samples were diluted in a saturated NFOH solution until the concentration of 4 nL/mL was achieved. Approximately 500 µL of this solution was injected into the NanoSight NS300 (Malvern Panalytical, UK) sample holder. Experiments were performed in triplicate with a duration of 60 s at a temperature of 25 °C using NTA software v3.1.

4.1.4. ZP

ZP was determined using Zetasizer ZS90 (Malvern Instruments, Malvern, UK) by the electrophoretic mobility method. The applied field force was 20 V/cm. ZP measurements were calculated in purified water with a conductivity adjusted to 50 µS.cm⁻¹ by adding 0.9% NaCl (*w/v*).

4.1.5. Lyophilization

Lyophilization was performed as follows: freezing the formulations at –45.0 °C, annealing with heating at –15 °C, and maintaining at that temperature for 1 h; primary drying at –30 °C shelf temperature and 75 mTorr pressure for 48 h and secondary drying at +25 °C shelf temperature under the same pressure for 4 h. The lyophilized formulations were used for biological activity assays.

4.1.6. XRD

XRD was performed to detect the crystallinity of pure NFOH and lyophilized NFOH nanosuspension. The powder was placed in a sample holder and scanned between 10° and 80° (2θ), exposed to CuKα radiation 40 kV and step time of 0.01.

4.2. Biology

4.2.1. Cytotoxicity on Macrophages (CC₅₀)

A suspension of 8×10^5 murine peritoneal macrophages in RPMI 1640 medium and bovine fetal serum (BFS) at 10.0% (inactivated by heat treatment), besides 1.0% penicillin (10,000 UI/mL)/streptomycin (10 mg/mL), which were placed to each well in 96-well plates. For cell adhesion, the macrophages plated were incubated in 5.0% CO₂ air mixture at 37 °C. Non-adherent cells were removed, after 24 h, by washing with RPMI 1640 medium. Then, compounds (NFOH-F1 and NFOH-F2) and reference drugs were added to the wells

containing the cells in different concentrations, ranging from 3.91 to 500.00 µg/mL in dimethyl sulfoxide (DMSO) with a final concentration of 0.6% (*v/v*), and the plates were incubated for another 48 h. Non-adherent cells were removed by washing with the RPMI 1640 medium. Then, 3-(4,5-dimethylthiazol-2-yl)-2,5-diphenyltetrazoliumbromide (MTT) was solubilized in phosphate-buffered saline (5.0 µg/mL), and 10 µL of it was added to the RPMI 1640 medium to make up a volume of 200.0 µL per well, followed by an incubation for 4 h [28]. Subsequently, the medium was removed, and 100.0 µL of DMSO was added to each well and homogenized for 15 min. Afterward, the absorbance of each well was calculated at 570 nm according to Equation (3) (OD represents optical density).

Equation (3).

$$\text{Inhibition} = (\text{OD}_{\text{control}} - \text{OD}_{\text{compounds}} / \text{OD}_{\text{control}}) \times 100 \quad (3)$$

Each experiment was performed in triplicate on three different days, and the cell culture control (medium + cells + DMSO 0.6% *v/v*) was used to calculate the percentage of viable cells and the determination of CC₅₀ values. The ratio of CC₅₀ and IC₅₀ values for amastigote forms were used to determine the selective index (SI).

4.2.2. In Vitro anti-*T. cruzi* Activity (IC₅₀)

The stock solutions of NFOH-F1, NFOH-F2, and BZN were solubilized in DMSO at 10 mg/mL. The epimastigotes (1.5 × 10⁶/mL per well) were incubated (BOD Incubators model) at 28 °C for 72 h. The analysis of those compounds were done in triplicate of seven doses, 200 µg/mL and a further six 2-fold serial dilutions. No effect against the epimastigotes was observed by the final DMSO concentration. Resazurin (1 mM) was added to each well, after incubation period. Absorbance at 570 nm and 600 nm were measured after 12 h of incubation with resazurin. The formula used to calculate the percentage of the epimastigotes proliferation inhibition was the following: % inhibition = 100 – [A₅₇₀ – (A₆₀₀ × R₀) Treated / A₅₇₀ – (A₆₀₀ × R₀) Control+] × 100, where A₅₇₀ = absorbance at 570 nm, A₆₀₀ = absorbance at 600 nm, Control+ = positive control: well containing culture medium, resazurin and epimastigotes without treatment, Control- = negative control: well containing only the culture medium and resazurin, without epimastigotes and treatment; R₀ = absorbance of the negative control [R₀ = (A₅₇₀ / A₆₀₀) Control-] [29]. For the antitrypomastigote assay, the parasites (1 × 10⁶) were incubated for 24 h, with the same concentrations of the evaluated compounds. The rates of parasite death were quantified by light microscopy. The IC₅₀ values of the compounds were calculated for both antiepipimastigote and antitrypomastigote assays at the CalcuSyn software (Biosoft, Cambridge, UK).

For analyzing the effects of NFOH-F1, NFOH-F2, or BZN against intracellular parasites in a 72 h assay, cells from neonatal rat cardiomyoblasts (1 × 10⁴ cells) of the H9c2 lineage (American Type Culture Collection, ATCC: CRL 1446) were incubated for 24 h in DMEM medium supplemented with 0.2% gentamicin (200 µg/mL), 1% glutamine 2 nM, and 10% FBS). After that, the cells were infected with trypomastigotes at a ratio of 20 parasites to 1 H9c2 cell and the plate were incubated for 24 h. Then, the treatment with the compounds NFOH-F1, NFOH-F2, or BZN at the following concentrations 120 µM, 60 µM, 30 µM, 15 µM, 7.5 µM, 3.75 µM, and 1.87 µM were done for three days. All tissue culture plate incubations were done at 37 °C and in a 5% CO₂-air mixture. After that, the cultures were fixed with methanol, stained with Giemsa, and the percentages of infected cells were estimated through a microscopy analysis of the treated and untreated cultures. The percentage of growth inhibition was calculated by the following formula: number of infected cells in the treated cultures / mean value of infected cell in the infected control cultures × 100. [30]. The IC₅₀ values were calculated using the CalcuSyn software.

4.2.3. In Vitro Anti-Leishmania Activity (IC₅₀)

The promastigotes of *L. amazonensis* (strain MHOM/BR/71973/M2269) were cultivated on 24-well plates in LIT medium supplemented with BFS at 10.0% (inactivated by heat

treatment) and 1.0% penicillin (10,000 UI/mL)/streptomycin (10.0 mg/mL) (Sigma, USA). In the logarithmic phase of the proliferation curve, cells were harvested and suspended in fresh medium, counted using Neubauer chambers, and adjusted to a concentration of 1×10^6 cells/mL using 24-wells plates. The compounds NFOH-F1 and NFOH-F2, in concentrations ranging from 0.10–40.00 $\mu\text{g/mL}$, were solubilized in DMSO (0.6% *v/v* in all wells), added to the promastigote cultures (1×10^6 cells/mL), and incubated at 25 °C. The remaining parasites were counted in a Neubauer chamber and compared with controls DMSO (0.6% *v/v*) to calculate IC_{50} [31], after 72 h of incubation. Amphotericin B (Sigma) was used as a reference drug and all tests were performed in triplicate at three different times.

Murine peritoneal macrophages were cultivated in RPMI 1640 medium (Sigma, USA) supplemented with BFS at 10.0% (inactivated by heat treatment) at 37 °C in 5.0% CO_2 incubator (project number 59/2017) for the assays with amastigote forms. In a 24-well plate chamber plus 13-mm glass slides (Nunc, Thermo Fischer Scientific Massachusetts-USA), the cells with a density of 8×10^5 cells per well were cultured. The macrophages were infected with late log-phase promastigotes at a ratio of 10:1 (parasite/macrophage), followed of incubation at 37 °C in 5.0% CO_2 incubator for 24 h (Espuri et al., 2019). Non-phagocytosed promastigote forms were removed by washing, and NFOH-F1 and NFOH-F2, in the concentrations 0.10–40.00 $\mu\text{g/mL}$, were administered after solubilization in DMSO at a concentration of 0.6% *v/v*. Absolute methanol was used, after 72 h, to fix the cells in the chamber slide, which were stained with 10.0% Giemsa, followed by examination in optical light microscope plus oil immersion. At least 200 macrophages were counted for the calculation of the percentage of infected cells per well. The ratio of inhibition (IC_{50} value) was calculated regarding the control with DMSO. Amphotericin B (Sigma) was used as a reference drug and all tests were performed in triplicate at three different times.

4.2.4. Anti-*T. cruzi* Murine Assay

Female Swiss mice (N = 20; n = 5) at about five weeks of age (20–25 g) were purchased from the Universidade Federal de Alfenas. The experiment was done in an ambient with control of temperature and water and food ad libitum. Blood trypomastigotes (5×10^3) of the *T. cruzi* Y strain were intraperitoneally inoculated. *T. cruzi* Y strain is known to have induce high level of parasitemia, 100% mortality when non-treated, and to be partially resistant to BZN. Tail blood was examined for the presence of parasites at four days post-infection (dpi). Only when trypomastigotes were detected in microscopy analysis, was the treatment started (5 dpi) [30]. The treatment drug was administered orally at 100 mg kg^{-1} . NFOH-F1, NFOH-F2, and BZN were diluted using distilled water with 5% de Cremophor (Sigma). The animals were treated by 200 μL of the compound suspensions through gavage at 5–9 dpi. Parasitemia and mortality were checked every day until 15 dpi. The protocol was approved by the Research Ethics Commission of the UNIFAL-MG (project number 59/2017) and was performed per the Guide for the Care and Use of Laboratory Animals.

4.3. Statistical Analysis

The 5% significance level ($p < 0.05$) was determined by Tukey multiple comparisons and ANOVA. GraphPad Prism (v. 8.1) was used for ANOVA.

5. Conclusions

The NFOH nanocrystals described in the present study (NFOH-F1 and NFOH-F2) exhibited similar activities compared with free NFOH [14–17]. Likewise, considering the fact that the NFOH nanocrystals can be tested against other strains of *T. cruzi* or Leishmania in animal assays, the present results are important to future studies on NFOH (free, nanocrystals, or polymers). Therefore, future studies with these potent novel anti-parasitic formulations should involve assays in both stages of Chagas disease and toxicity assays in mice to assess their cytotoxicity.

In conclusion, NFOH-F1 and NFOH-F2 exhibit similar effects as free NFOH and BZN, indicating their potent effects on the short acute stage of experimental Chagas disease in a murine model. Thus, both formulations (NFOH-F1 and NFOH-F2) can be promising drug candidates for future analysis against trypanosomatid parasites.

Author Contributions: C.B.S., A.d.S., D.S.S.M., E.G.d.S., L.d.F.D.C., I.S.C., P.F.E., M.J.M., E.I.F., N.A.B.-C. and C.M.C. designed the experiments and analyzed the data. C.B.S., A.d.S., D.S.S.M., E.G.d.S., L.d.F.D.C. and P.F.E. performed the experiments. C.B.S. wrote the manuscript, with input from I.S.C., M.J.M., E.I.F., N.A.B.-C. and C.M.C. All authors have read and agreed to the published version of the manuscript.

Funding: The authors would like to thank the Fundação de Amparo à Pesquisa do Estado de São Paulo (FAPESP-2016/10847-9) for assistance in the form of research fellowships. This work was financed in part by the Coordenação de Aperfeiçoamento Pessoal de Nível Superior-Brasil (CAPES), finance code: 001.

Institutional Review Board Statement: This study was carried out in strict accordance with the recommendations in the UNIFAL Guide for the Care and Use of Laboratory Animals.

Informed Consent Statement: Not applicable.

Data Availability Statement: The data supporting the findings of the research article is available within this article.

Acknowledgments: The authors would like to thank the Programa de Apoio ao Desenvolvimento Científico da Faculdade de Ciências Farmacêuticas da UNESP (PADC/FCF-UNESP).

Conflicts of Interest: The authors declare no conflict of interest.

References

1. WHO-World and Health Organization. Neglected Tropical Diseases. Available online: www.who.int/neglected_diseases/diseases/en/ (accessed on 6 December 2022).
2. DNDi. Drugs for Neglected Diseases Initiative (DNDi), Neglected Tropical Diseases-Chagas Disease. 2020. Available online: <https://www.dndi.org/diseases-projects/chagas/> (accessed on 6 December 2022).
3. Alvar, J.; Croft, S.; Olliaro, P. Chemotherapy in the treatment and control of leishmaniasis. *Adv. Parasitol.* **2006**, *61*, 223–274. [[PubMed](#)]
4. Andrade, M.C.; Oliveira, M.D.F.; Nagao-Dias, A.T.; Coêlho, I.C.B.; Cândido, D.D.S.; Freitas, E.C.; Bezerra, F.S.M. Clinical and serological evolution in chronic Chagas disease patients in a 4-year pharmacotherapy follow-up: A preliminary study. *Rev. Soc. Bras. Med. Trop.* **2013**, *46*, 776–778. [[CrossRef](#)] [[PubMed](#)]
5. Barrett, M.P.; Croft, S.L. Management of trypanosomiasis and leishmaniasis. *Br. Med. Bull.* **2012**, *104*, 175–196. [[CrossRef](#)] [[PubMed](#)]
6. Castro, J.A.; DeMecca, M.M.; Bartel, L.C. Toxic side effects of drugs used to treat chagas' disease (american trypanosomiasis). *Hum. Exp. Toxicol.* **2006**, *25*, 471–479. [[CrossRef](#)] [[PubMed](#)]
7. Fernandez, M.L.; Marson, M.E.; Ramirez, J.C.; Mastrantonio, G.; Schijman, A.G.; Altcheh, J.; Riarte, A.R.; Bournissen, F.G. Pharmacokinetic and pharmacodynamic responses in adult patients with Chagas disease treated with a new formulation of benznidazole. *Memórias Do Inst. Oswaldo Cruz* **2016**, *111*, 218–221. [[CrossRef](#)]
8. Fuentes, B.R.; Maturana, A.M.; Cruz, M.R. Eficacia de nifurtimox para el tratamiento de pacientes con enfermedad de Chagas cronica. *Rev. Chil. Infectol.* **2012**, *29*, 82–86. [[CrossRef](#)]
9. Maya, J.D.; Orellana, M.; Ferreira, J.; Kemmerling, U.; López-Muñoz, R.; Morello, A. Chagas disease: Present status of pathogenic mechanisms and chemotherapy. *Biol. Res.* **2010**, *43*, 323–331. [[CrossRef](#)]
10. McGwire, B.S.; Satoskar, A.R. Leishmaniasis: Clinical syndromes and treatment. *Mon. J. Assoc. Phys.* **2014**, *107*, 7–14. [[CrossRef](#)]
11. WHO-World and Health Organization. Control of Chagas disease: Second report of the WHO expert committee World Health Organization (2000: Brasilia, Brazil). *Geneva World Health* **2002**, *905*, 109.
12. Scarim, C.B.; Chung, M.C. Current Approaches of Drug Discovery for Chagas Disease: Methodological Advances. *Comb. Chem. High Throug. Screen.* **2019**, *22*, 1–12. [[CrossRef](#)]
13. Scarim, C.B.; Jornada, D.H.; Chelucci, R.C.; De Almeida, L.; Dos Santos, J.L.; Chung, M.C. Current advances in drug discovery for Chagas disease. *Eur. J. Med. Chem.* **2018**, *5234*, 30531. [[CrossRef](#)] [[PubMed](#)]
14. Chung, M.C.; Güido, R.V.C.; Martinelli, T.F.; Gonçalves, M.F.; Carneiro Poll, M.; Botelho, K.C.A.; Ferreira, E.I. Synthesis and in vitro evaluation of potential antichagasic hydroxymethylnitrofurazone (NFOH-121): A new nitrofurazone prodrug. *Bioorg. Med. Chem.* **2003**, *11*, 4779–4783. [[CrossRef](#)] [[PubMed](#)]

15. Scarim, C.B.; Olmo, F.; Ferreira, E.I.; Chung, M.C.; Kelly, J.M.; Francisco, A.F. Image-Based In vitro Screening Reveals the Trypanostatic Activity of Hydroxymethylnitrofurazone against *Trypanosoma cruzi*. *Int. J. Mol. Sci.* **2021**, *22*, 6930. [[CrossRef](#)] [[PubMed](#)]
16. Davies, C.; Cardozo, R.M.; Negrette, O.S.; Mora, M.C.; Chung, M.C.; Basombrio, M.A. Hydroxymethylnitrofurazone is active in a murine model of Chagas' disease. *Antimicrob. Agents Chemother.* **2010**, *54*, 3584–3589. [[CrossRef](#)]
17. Scarim, C.B.; de Andrade, C.R.; da Rosa, J.A.; dos Santos, J.L.; Chung, M.C. Hydroxymethylnitrofurazone treatment in indeterminate form of chronic Chagas disease: Reduced intensity of tissue parasitism and inflammation—A histopathological study. *Int. J. Exp. Pathol.* **2018**, *99*, 236–248. [[CrossRef](#)] [[PubMed](#)]
18. Davies, C.; Dey Negrett, O.S.; Parada, L.A.; Basombrio, M.A.; Garg, N.J. Hepatotoxicity in Mice of a Novel Anti-parasite Drug Candidate Hydroxymethylnitrofurazone: A Comparison with Benznidazole. *PLoS Negl. Trop. Dis.* **2014**, *8*, e3231. [[CrossRef](#)]
19. Chen, M.L.; John, M.; Lee, S.L.; Tyner, K.M. Development Considerations for Nanocrystal Drug Products. *AAPS J.* **2017**, *19*, 642–651. [[CrossRef](#)]
20. Müller, R.H.; Gohla, S.; Keck, C.M. State of the art of nanocrystals-Special features, production, nanotoxicology aspects and intracellular delivery. *Eur. J. Pharm. Biopharm.* **2011**, *78*, 1–9. [[CrossRef](#)]
21. Noyes, A.A.; Whitney, W.R. The rate of solution of solid substances in their own solutions. *J. Amer. Chem. Soc.* **1897**, *19*, 930–934. [[CrossRef](#)]
22. Doriguetto, A.C.; de Paula Silva, C.H.; Ellena, J.; Trossini, G.H.; Chin, C.M.; Ferreira, E.I. 5-Nitro-2-furaldehyde *N*-(hydroxymethyl) semicarbazone. *Acta Crystallogr. Sect. E Struct. Rep. Online* **2005**, *61*, 2099–2101. [[CrossRef](#)]
23. Varshosaz, J.A.; Talari, R.; Mostafavi, S.A.; Nokhodchi, A. Dissolution enhancement of gliclazide using in situ micronization by solvent change method. *Powder Technol.* **2008**, *187*, 222–230. [[CrossRef](#)]
24. De Souza, A.; Marin, D.S.S.; Mathias, S.L.; Monteiro, L.M.; Yukuyama, M.N.; Scarim, C.B.; Bou-Chacra, N.A. Promising nanotherapy in treating leishmaniasis. *Intern. J. Pharm.* **2018**, *547*, 421–431. [[CrossRef](#)] [[PubMed](#)]
25. Morilla, M.J.; Romero, E.L. Nanomedicines against Chagas disease: An update on therapeutics, prophylaxis and diagnosis. *Nanomedicine* **2015**, *10*, 465–481. [[CrossRef](#)] [[PubMed](#)]
26. Monteiro, L.M.; Löbenberg, R.; Ferreira, E.I.; Cotrim, P.C.; Kanashiro, E.; Rocha, M.; Chung, C.M.; Bou-Chacra, N.A. Targeting *Leishmania amazonensis* amastigotes through macrophage internalisation of a hydroxymethylnitrofurazone nanostructured polymeric system. *Int. J. Antimicrob. Agents* **2017**, *50*, 88–92. [[CrossRef](#)] [[PubMed](#)]
27. Romero, G.B.; Keck, C.M.; Muller, R.H.; Bou-Chacra, N.A. Development of cationic nanocrystals for ocular delivery. *Eur. J. Pharmac. Biopharmac.* **2016**, *107*, 215–222. [[CrossRef](#)] [[PubMed](#)]
28. Mosmann, T. Rapid colorimetric assay for cellular growth and survival: Application to proliferation and cytotoxic assays. *J. Immunol. Methods* **1983**, *65*, 55–63. [[CrossRef](#)]
29. Rolón, M.; Vega, C.; Escario, J.A.; Gómez-Barrio, A. Development of resazurin microtiter assay for drug sensibility testing of *Trypanosoma cruzi* epimastigotes. *Parasitol. Res.* **2006**, *99*, 103–107. [[CrossRef](#)]
30. Brancaglioni, G.A.; Toyota, A.E.; Cardoso Machado, J.V.; Fernandes Júnior, A.Á.; Silveira, A.T.; Vilas Boas, D.F.; Carvalho, D.T. In vitro and in vivo trypanocidal activities of 8-methoxy-3-(4-nitrobenzoyl)-6-propyl-2*H*-cromen-2-one, a new synthetic coumarin of low cytotoxicity against mammalian cells. *Chem. Biol. Drug Des.* **2018**, *92*, 1888–1898. [[CrossRef](#)]
31. Espuri, P.F.; Dos Reis, L.L.; Peloso, E.F.; Gontijo, V.S.; Colombo, F.A.; Nunes, J.B.; de Oliveira, C.E.; de Almeida, E.T.; Silva, D.E.S.; Bortoletto, J.; et al. Synthesis and evaluation of the antileishmanial activity of silver compounds containing imidazolidine-2-thione. *J. Biol. Inorg. Chem.* **2019**, *24*, 419–432. [[CrossRef](#)]